First-principles investigations of elastic properties and energetics of antiferroelectric and ferroelectric phases of $PbZrO_3$

R. Kagimura
Materials Science and Technology Division, Oak Ridge National Laboratory, Oak Ridge, Tennessee 37831-6114, USA and Department of Physics and Astronomy, University of Tennessee, Knoxville, Tennessee 37996-1200, USA

D. J. Singh
Materials Science and Technology Division, Oak Ridge National Laboratory, Oak Ridge, Tennessee 37831-6114, USA

(Received 8 October 2007; revised manuscript received 26 December 2007; published 14 March 2008)

We report an *ab initio* study of the elastic properties and energetics of the orthorhombic (AFO) and rhombohedral (RF) phases of $PbZrO_3$. We report the polarization for the RF phase and the elastic constants, the sound velocity, and the total energy for both phases. Our results show that the two phases are energetically close, by 2.3 mRy per formula unit, and the AFO phase is the most stable one consistent with the experimental phase diagram. The elastic constant and sound velocity calculations show that depending on the orientation, either phase can be the effectively stiffer one and that these differences are large. This suggests that control of the balance between these phases via strain is possible, for example, in epitaxy and in particular that the ferroelectric state can be stabilized even without lattice dilation.

DOI: 10.1103/PhysRevB.77.104113 PACS number(s): 77.80.Fm, 77.84.Dy, 62.20.D−, 71.15.Mb

I. INTRODUCTION

The perovskite solid solution of $PbZrO_3$ and $PbTiO_3$, which is known as PZT, has been widely investigated[1–3] for many years due to its useful piezoelectric and ferroelectric properties. The PZT phase diagram[1] is very rich. PZT is generally ferroelectric with a Curie temperature that decreases gradually with Zr concentration. It shows several different ferroelectric phases including large rhombohedral ferroelectric and tetragonal ferroelectric regions separated by the so-called morphotropic phase boundary (MPB). However, pure $PbZrO_3$ (PZ) has an antiferroelectric orthorhombic structure, which persists for a very narrow composition range in the PZT phase diagram. There is a low-temperature phase transition from this antiferroelectric orthorhombic (AFO) phase to the rhombohedral ferroelectric (RF) phase at about 7% Ti concentration. A transition from the RF phase to the AFO phase can also be induced by applying modest hydrostatic pressure.[4] It has been shown, by several experimental works,[5–15] that a phase switching between the AFO phase to the RF phase is possible. This arises because electric field couples to polarization and therefore favors the RF phase. Also, some experimental investigations have shown that the stabilization of the ferroelectric state in thin films is possible, presumably related to stress effects.[7,9] A rhombohedral phase was reported for the end-point compound, PZ,[16] in a narrow temperature range around 230 °C. In any case, it may be presumed that the RF phase is close in energy to the AFO phase based on their proximity in the PZT phase diagram and on theoretical results.[17,18]

Both the RF and AFO phases may be viewed as distortions of the "perfect" cubic perovskite structure. However, these distortions are large in Zr rich PZT and so these two phases are rather different from a structural point of view, even though they are close energetically. *Ab initio* calculations show, for PZ, that the energy gain, due to these distortions, is ≈0.25 eV/Pb (Ref. 19) relative to the "perfect" cubic perovskite. The AFO phase has large octahedral tilts,[20,21] while the RF phase of PZT has a different pattern of tilts and a large polarization characteristic of large ferroelectric displacements of the atoms.[22] Therefore the AFO and RF phases may present quite different elastic behavior, and as they are energetically close, the understanding of how strains affect the energetic balance between these two phases is important in the development of devices that use the antiferroelectric/ferroelectric switching, as well as in physics of multilayer systems,[23] where strain effects can be very important in stabilizing phases other than the bulk ground state.[24]

The purpose of this paper is to explore this balance and to report calculations of elastic constants. Even though elastic properties have been reported by several first-principles calculations, as well as many experimental works for different materials, including $PbTiO_3$,[25,26] elastic properties are difficult to measure for PZ and PZT bulk, due to the twinning[27] of these materials and the difficulty in synthesizing suitable crystals for measurements. Moreover, the RF phase of pure PZ is experimentally inaccessible. Nevertheless, PZ thin films free of twin structures[28] can be grown.

Here, we report calculations of the elastic constants for the RF and AFO PZ phases using a direct first-principles total energy approach. This yields the bulk modulus, as well as the sound velocities as a function of direction. The total energy calculations were performed using an all-electron full potential linearized augmented plane wave (LAPW) method. We calculated the total polarization for the RF phase using Berry phase theory. Our results show that the AFO phase is more stable than the RF one by 2.3 mRy/Pb. The calculated polarization of the RF phase is 55 $\mu C/cm^2$. The sound velocity calculations show very different elastic anisotropies of the two phases and, depending on the orientation, either phase can be the stiffer of the two. This suggests that control via strain can be possible, for example, in epitaxy and that it may favor the ferroelectric state, even without lattice dilation.

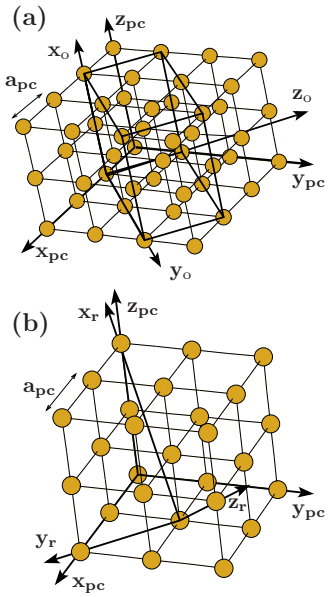

FIG. 1. (Color online) Coordinate systems used in our calculations for the (a) orthorhombic and (b) rhombohedral structures and their relation to that of the pseudocubic cell. The indices "pc," "o," and "f" refer to the pseudocubic, orthorhombic, and rhombohedral cells, respectively. The solid circles represent the Pb atoms and $\mathbf{a_{pc}}$ is the pseudocubic lattice constant.

II. FIRST-PRINCIPLES CALCULATIONS

Our calculations were performed in the framework of the density functional theory (DFT),[29] within the local density approximation (LDA).[30] The total energy calculations were done using the general potential linearized augmented plane wave (LAPW) method[31] with local orbitals[32] as implemented in our in-house code. The sphere radii used in the LAPW method were 2.20, 2.00, and 1.60 a.u. for Pb, Zr, and O, respectively. We used a LAPW cutoff $RK_{\max}=7.0$, where R is the smallest LAPW sphere radius. The total energy differences are converged to a precision of better than 1 mRy per formula unit. All atomic positions were fully relaxed in the LAPW calculations. To perform the total electric polarization calculations, we have used the geometric Berry phase theory,[33] implemented in the SIESTA code,[34] which is a code based on an *ab initio* method that uses a local basis set for the one electron wave functions and pseudopotentials.[35] In this calculation, we have used the atomic positions obtained in the LAPW calculations. We used **k** points[36] meshes of $4\times4\times4$ and $4\times2\times4$ for the integration in the Brillouin zone for the ten atoms per cell rhombohedral and 40 atoms per cell orthorhombic structures, respectively, for both methods.

As mentioned, the AFO structure is the ground state of $PbZrO_3$. It has a 40 atom cell, whose relationship to the ideal cubic cell is defined by its lattice vectors of approximately $(0,0,2)a_{pc}$, $(2,2,0)a_{pc}$, and $(\bar{1},1,0)a_{pc}$, where a_{pc} is the pseudocubic lattice constant. The orthorhombic cell related to the pseudocubic cell is shown in the Fig. 1(a). The atomic positions for the Pb, Zr, and O atoms for this structure were calculated previously[19] and shown to be in excellent agreement with experiments.[20] In fact, LDA calculations were shown to be predictive in this material, in that they yielded a structure different from the existing literature structures, but which was subsequently verified by neutron diffraction.[20]

Regarding the rhombohedral cell, which is defined by the lattice vectors, in the pseudocubic coordinate system, $(0,1,1)a_{pc}$, $(1,0,1)a_{pc}$, and $(1,1,0)a_{pc}$, there is no experimental data about its lattice constant because it is not the most stable PZ phase. We start with a pseudocubic lattice with 10 atoms/cell ($R3c$ space group), which is a rhombohedron along the [111] direction. This structure is the same as the phase that occurs with small Ti addition. The initial pseudocubic lattice constant was obtained by constraining the pseudocubic volume per formula unit to be equal to that of the orthorhombic lattice.

III. RESULTS AND DISCUSSIONS

A. Elastic properties

Let us first address the calculations of the (second order) elastic constants, C_{ijkl}, for the orthorhombic and rhombohedral structures. The C_{ijkl} can be defined using an expansion of the total energy, $E(V,\delta)$, of a strained system of volume V in a Taylor series with respect to a distortion parameter δ. Keeping until the third term in the Taylor series, since we have considered only small lattice distortions in our calculations, $E(V,\delta)$ is written as[37]

$$E(V,\delta)=E_0+V_0\left(\sum_{i,j}\tau_{ij}\delta_{ij}+\frac{1}{2}\sum_{i,j,k,l}C_{ijkl}\delta_{ij}\delta_{kl}\right), \quad (1)$$

where: E_0 is the total energy of an unstrained system of volume V_0, τ is the stress tensor matrix, δ_{ij} is an element in the distortion matrix, and the indices i, j, k, and l run over the x, y, and z.

The strained lattice vectors are obtained by multiplying the lattice vectors of the unstrained system by the distortion matrix, which is symmetric ($\delta_{ij}=\delta_{ji}$) and can be written as

$$\begin{pmatrix}1+\delta_{xx} & \delta_{xy} & \delta_{xz}\\ \delta_{yx} & 1+\delta_{yy} & \delta_{yz}\\ \delta_{zx} & \delta_{zy} & 1+\delta_{zz}\end{pmatrix}. \quad (2)$$

For the unstrained orthorhombic lattice, we have used the experimental values for the lattice constants,[38] that is, $a=8.2077$ Å, $b=11.7742$ Å, and $c=5.8752$ Å. So, the V_0 used in Eq. (1) is 70.97 Å^3/Pb, which is 3% larger than the theoretical (LDA) volume, 68.86 Å^3/Pb. This can change the value for the elastic constant by 3%. For the unstrained rhombohedral lattice, we have used a pseudocubic lattice, which is a rhombohedron along the [111] direction and with a rhombohedral angle α_{rh}. To calculate this rhombohedral angle we have performed total energy calculations. To do that, since the total energy is dependent of the volume, we have kept the volume per formula unit constant and equal to that of the orthorhombic cell, varied the rhombohedral angle from 58.40° to 60.80°, and calculated the total energy. Our results indicate that the rhombohedral angle that minimizes the total energy is equal to 59.5°. This structure is energetically very close (by ≈0.2 mRy/Pb) to that one with α_{rh}

TABLE I. Matrix elements, δ_{ij}, of the distortion matrices [Eq. (2)] we have used in our calculations, and the corresponding second order coefficients of Eq. (1) (see text).

Orthorhombic						
δ_{xx}	δ_{yy}	δ_{zz}	δ_{xy}	δ_{xz}	δ_{yz}	Second order coefficient
δ	0	0	0	0	0	$(C_{11}/2)$
0	δ	0	0	0	0	$(C_{22}/2)$
0	0	δ	0	0	0	$(C_{33}/2)$
0	0	0	0	0	δ	$(2C_{44})$
0	0	0	0	δ	0	$(2C_{55})$
0	0	0	δ	0	0	$(2C_{66})$
δ	$-\delta$	0	0	0	0	$[(C_{11}/2)+(C_{22}/2)-C_{12}]$
δ	0	$-\delta$	0	0	0	$[(C_{11}/2)+(C_{33}/2)-C_{13}]$
0	δ	$-\delta$	0	0	0	$[(C_{22}/2)+(C_{33}/2)-C_{23}]$
Rhombohedral						
δ	δ	0	0	0	0	$(C_{11}+C_{12})$
δ	$-\delta$	0	0	0	0	$(C_{11}-C_{12})$
0	0	δ	0	0	0	$(C_{33}/2)$
0	0	0	0	0	δ	$(2C_{44})$
δ	δ	δ	0	0	0	$[C_{11}+(C_{33}/2)+C_{12}+2C_{13}]$
δ	$-\delta$	0	0	0	δ	$(C_{11}-C_{12}+2C_{44}+4C_{14})$

$=60°$, which corresponds to an fcc lattice as far as the translational symmetry is concerned. As this energy difference is very small and is in the range of the numerical errors, we consider in our calculations the RF unstrained structure with $\alpha_{rh}=60°$ and $a=4.140\ 27$ Å, which was obtained using the $V_{\mathrm{AFO}}=V_{\mathrm{FR}}$ constraint. To represent the rhombohedral lattice we have used the lattice vectors of a corresponding hexagonal lattice: $\vec{a}_1^H$, $\vec{a}_2^H$, and $\vec{c}$. Then, we strain the hexagonal lattice vectors using Eq. (2), and we find the corresponding fcc lattice vectors ($\vec{a}_1$, $\vec{a}_2$, and $\vec{a}_3$), which match those distorted hexagonal vectors, using the following relations: $\vec{a}_1^H=(\vec{a}_1-\vec{a}_2)$, $\vec{a}_2^H=(\vec{a}_2-\vec{a}_3)$, and $\vec{c}^H=(\vec{a}_1+\vec{a}_2+\vec{a}_3)$, where $\vec{a}_1=(0,1,1)a$, $\vec{a}_2=(1,0,1)a$, and $\vec{a}_3=(1,1,0)a$.

The orthorhombic phase has nine distinct elastic constants, referred to as C_{11}, C_{22}, C_{33}, C_{12}, C_{13}, C_{23}, C_{44}, C_{55}, and C_{66}; while the rhombohedral phase ($R3c$ space group) has six distinct elastic constants, that is, C_{11}, C_{33}, C_{12}, C_{13}, C_{44}, and C_{14}. Here, we have used the Voight notation, where the indices xx, yy, zz, yz or zy, xz or zx, and xy or yx are replaced by 1, 2, 3, 4, 5, and 6, respectively. Also, we have used the following convention[39] for the x,y,z coordinate system: for the orthorhombic lattice we consider the x, y, and z axes parallel to a, b, and c, respectively, with $c<a<b$, as shown in Fig. 1(a). For the rhombohedral structure, we choose the z and y axes along the [111] and $[1\bar{1}0]$ directions of the pseudocubic lattice, respectively, as shown in Fig. 1(b).

In order to calculate the elastic constants, we have considered nine (six) distinct distortion matrices for the orthorhombic (rhombohedral) structure. The matrix elements for each distortion matrix we have used are shown in the Table I. From Eq. (1), we observe that the second order coefficient is a linear combination of elastic constants. For example, to calculate C_{11} of the AFO structure, we have used the following distortion matrix:

$$\begin{pmatrix} 1+\delta & 0 & 0 \\ 0 & 1 & 0 \\ 0 & 0 & 1 \end{pmatrix}.$$

Using this distortion matrix in Eq. (1), we obtain the following expression for the total energy: $E(V,\delta)=E_0+V_0(\tau_1\delta+\frac{1}{2}C_{11}\delta^2)$. The second order coefficient related to this distortion is $C_{11}/2$. Then, performing total energy *ab initio* calculations for each distortion matrix, and allowing a full relaxation of the atomic positions, we obtain $E(V,\delta)$ for several values of δ ranging from -0.02 to 0.02, for example $\delta_1=-0.01$, $\delta_2=0.00$, $\delta_3=0.01$, and so on. The calculated total energies $[E(\delta_1), E(\delta_2), E(\delta_3),\ldots]$ are fitted by a third order polynomial, $E(\delta)=k_0+k_1\delta+k_2\delta^2+k_3\delta^3$, where k_0, k_1, k_2, and k_3 are the polynomial coefficients. Comparing the fitted equation to Eq. (1), we observe that the k_2 coefficient, which is determined by *ab initio* calculations, is equal to the second order coefficient of Eq. (1), shown in Table I.

In Table II, we show the calculated elastic constants for the orthorhombic and rhombohedral structures. The fitting error that we find is $\approx 3\%$. Thus the error of our calculated elastic constants is likely $\approx 5\%$, consistent with other LDA calculations (see, e.g., Refs. 37 and 40).

Now, using the calculated elastic constants, we obtain the bulk modulus, B, for both structures. The bulk modulus can be defined as the inverse of the volume compressibility (κ):[41]

$$B=\frac{1}{\kappa}=\frac{1}{S_{11}+S_{22}+S_{33}+2(S_{12}+S_{13}+S_{23})}, \qquad (3)$$

where S is the compliance matrix, which is defined as the inverse of the elastic constant matrix. Formulas relating ex-

TABLE II. Calculated elastic constants (C) and bulk modulus (B), in GPa, for the antiferroelectric orthorhombic and ferroelectric rhombohedral structures.

Orthorhombic		Rhombohedral	
C_{11}	210	C_{11}	229
C_{22}	264	C_{33}	150
C_{33}	158	C_{12}	72
C_{12}	83	C_{13}	64
C_{13}	53	C_{14}	13
C_{23}	85	C_{44}	117
C_{44}	75	B	107
C_{55}	55		
C_{66}	67		
B	111		

plicitly the bulk modulus for the orthorhombic and rhombohedral structures and the elastic constants can be found in Refs. 42 and 43.

In Table II, we show the results for the calculated bulk modulus for both structures. This table indicates that the bulk modulus for the rhombohedral structure is slightly smaller than that of the orthorhombic structure, indicating that the RF phase is slightly softer than the AFO phase, though this difference is not significant in view of the errors in our fits. Also, our result is in good agreement with the experimental result for antiferroelectric ceramic $PbZrO_3$, 122 GPa.[44]

B. Sound velocity

Even though the AFO and RF are distorted lattices based on the same cubic perovskite, they may as mentioned present quite different anisotropic elastic behavior because the distortions are strong. To study this elastic anisotropy, we now investigate how the stiffness varies in different directions of the AFO and RF phases. To investigate that, we calculate the sound velocity, v, for all directions using the Christoffel relation[45,46]

$$(C_{ijkl}n_j n_k - \rho v^2 \delta_{il})p_l = 0, \tag{4}$$

where the vector $\vec{n}$ indicates the direction of the wave propagation, ρ is the density of the material, δ_{il} is the Kronecker delta, p is the displacement vector, and the indices i, j, k, and l run over x, y, and z. To obtain the longitudinal and transverse velocities, we need to diagonalize the matrix Γ, which is defined as $\Gamma_{il}=\Sigma_{jk}C_{ijkl}n_j n_k$. To compare the results for the AFO and RF phases, we consider the same coordinate system for both structures. As the reference system, we have chosen the coordinate system of the pseudocubic perovskite structure, shown in Fig. 1. In this system, the x, y, and z axes

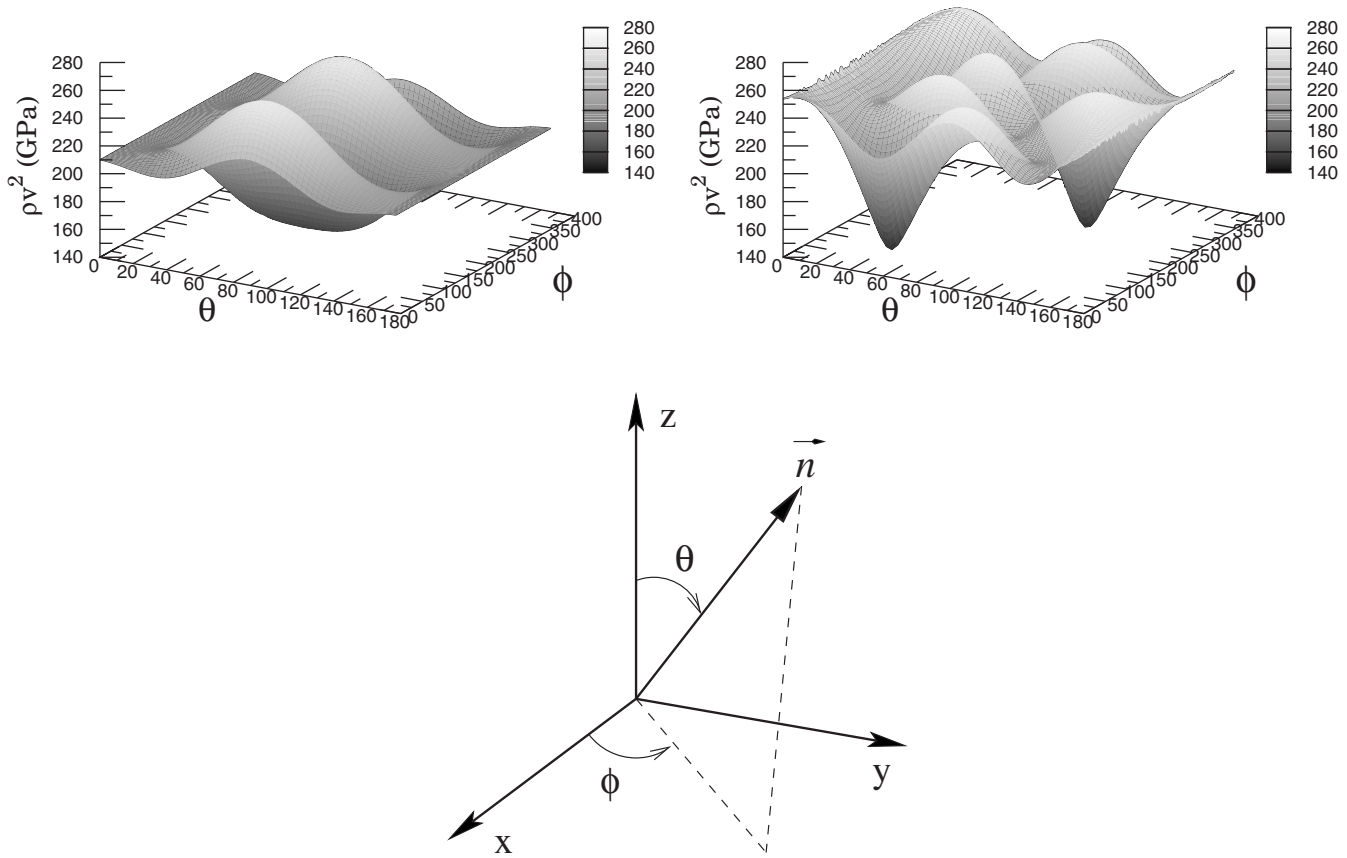

FIG. 2. Longitudinal velocities (v) for the orthorhombic (left) and rhombohedral (right) structures. We use the pseudocubic perovskite coordinate system, θ is the angle, in degrees, between the vector $\vec{n}$ and the z axis, and ϕ is the angle, in degrees, between the projection of the vector $\vec{n}$ onto the x-y plane and the x axis. ρ is the PZ mass density.

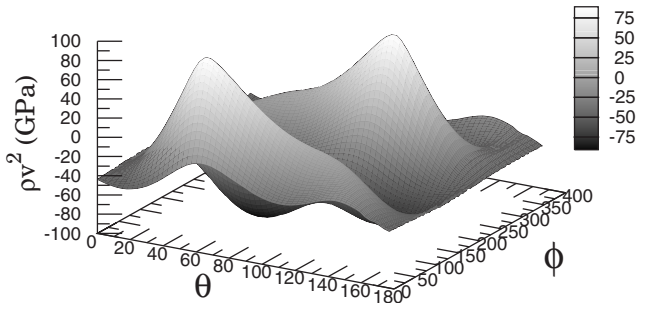

FIG. 3. Longitudinal velocities differences between the orthorhombic and rhombohedral structures.

of the orthorhombic lattice are along the [001], [110], and $[\bar{1}10]$ directions of the pseudocubic perovskite, respectively; while the z and y axes of the rhombohedral lattice are along the [111] and $[1\bar{1}0]$ directions, respectively.

In the Fig. 2, we show the results for the calculated longitudinal sound velocities for the AFO and RF structures. We used the cubic perovskite coordinate system, where θ is the angle between the z axis and the vector $\vec{n}$, and ϕ is the angle between the x axis and the projection of $\vec{n}$ onto the plane x-y, shown in the Fig. 2. Our results indicate that the square of the longitudinal sound speed multiplied by ρ ranges from 158 to 264 GPa for the AFO phase, and from 150 to 268 GPa for the RF one. Also, in this figure, we can note the anisotropic elastic behavior for both phases. The square of the transverse speed multiplied by ρ (not shown) ranges from 55 to 76 GPa, and from 59 to 121 GPa for the AFO and RF structures, respectively. Also, we plot the difference of the square of the longitudinal sound speed multiplied by ρ between the AFO and RF phases, and the results are shown in the Fig. 3. This figure shows that the difference ranges from −91 to 89 GPa. The region where the difference is negative indicates that the RF phase is stiffer than the AFO phase, while the region where it is positive indicates that the AFO phase is stiffer than the RF one. So, the above results show different elastic behavior for the AFO and RF structures, and suggest that depending on the orientation one phase can be stiffer or softer than the other one. Therefore as the total energy of strained systems depends on the elastic constants [see Eq. (1)], and either phase can be the effectively stiffer one depending on the orientation, our results indicate that a control via strain may favor one phase over the other. This result can explain the stabilization of the ferroelectric phase by stress effects observed in thin films.[7,9]

C. Energetics and polarization

So far, we have investigated the elastic properties of the AFO and RF phases. Turning to the energetics for these phases, we calculate the total energy as a function of the volume for both phases, using the distortion matrix: ($\delta_{xx}=\delta$, $\delta_{yy}=\delta$, $\delta_{zz}=\delta$, $\delta_{xy}=0$, $\delta_{xz}=0$, $\delta_{yz}=0$). As for the elastic constants calculation, the atomic positions were fully relaxed. The calculated strain-energy results were fitted by a third order polynomial and the total energy was minimized in relation to δ. Our results show that the orthorhombic phase is energetically more stable than the rhombohedral phase by 2.3 mRy per formula unit, while the corresponding energy minimizing volume for the rhombohedral and orthorhombic phases are quite similar, 69.3 and 68.9 Å^3, respectively. For the AFO phase, the shortest (longest) distance between the Zr and the nearest O atom ($d_{\text{Zr-O}}$) is 2.04 Å (2.15 Å), the shortest (longest) distance between the Pb and the nearest O atom ($d_{\text{Pb-O}}$) is 2.43 Å (3.41 Å), while the Zr-O-Zr angle ranges from 150° to 170°; for the RF phase, $d_{\text{Zr-O}}$ is equal to 2.03 Å (2.14 Å), $d_{\text{Pb-O}}$ is equal to 2.52 Å (3.32 Å), and the Zr-O-Zr angle is around 158°. Thus the off-centerings of the cations with respect to their cages are similar for both the ferroelectric and nonferroelectric structures.

To further investigate the energetic balance between those phases, we calculate the total polarization of the rhombohedral (ferroelectric) phase and the coupled electric field. The calculated total electric polarization is along the [111] direction of the cubic perovskite and its value is equal to 55 μC/cm^2. The calculated total polarization is in accord with the maximum polarization, 41 μC/cm^2, measured in PZ thin films.[13] The electric field ($\vec{E}$) needed to switch from antiferroelectric to ferroelectric phases in unstrained bulk can then be estimated using the total energy difference per unit formula volume (ΔU) and the above calculated polarization $\vec{P}$, using the relation $\Delta U=-\vec{P}\cdot\vec{E}$. This yields ≈1.3 MV/cm along the [111] direction of the cubic perovskite, which is only an estimate since it assumes that the polarizabilities are negligible.

IV. CONCLUSIONS

In conclusion, we studied the elastic properties and energetics of the AFO and RF phases of $PbZrO_3$. Our results show that the AFO and RF phases are energetically close and the AFO phase is more stable than the RF phase by 2.3 mRy/Pb. The elastic constant and sound velocity calculations show rather different elastic anisotropies of the two phases and that depending on the orientation, either phase can be the effectively stiffer one. So, as the total energy of strained systems depends on the elastic constants, our results indicate that a control via strain may favor one phase over the other. This implies that control of the balance between these two phases via strain is possible, for example, by epitaxy.

ACKNOWLEDGMENTS

This work was supported by the Department of Energy, ORNL LDRD program, and Division of Materials Science and Engineering, and by the Office of Naval Research. One of the authors (R.K.) also was supported by the Brazilian agency—CNPq.

[1] B. Jaffe, W. R. Cook, and H. Jaffe, *Piezoelectric Ceramics* (Academic, New York, 1971).
[2] K. Uchino, *Piezoelectric Actuators and Ultrasonic Motors* (Kluwer Academic, Dordrecht, 1971).
[3] E. Cross, Nature (London) **432**, 24 (2004).
[4] M. Avdeev, J. D. Jorgensen, S. Short, G. A. Samara, E. L. Venturini, P. Yang, and B. Morosin, Phys. Rev. B **73**, 064105 (2006).
[5] G. Shirane, E. Sawaguchi, and Y. Takagi, Phys. Rev. **84**, 476 (1951).
[6] I. Kanno, S. Hayashi, M. Kitagawa, R. Takayama, and T. Hirao, Appl. Phys. Lett. **66**, 145 (1995).
[7] T. Tani, J. Li, D. Viehland, and D. A. Payne, J. Appl. Phys. **75**, 3017 (1994).
[8] K. Yamakawa, S. Trolier-McKinstry, J. P. Dougherty, and S. B. Krupanidhi, Appl. Phys. Lett. **67**, 2014 (1995).
[9] B. Xu, Y. Ye, and L. E. Cross, J. Appl. Phys. **87**, 2507 (2000).
[10] M. P. Moret, J. J. Schermer, F. D. Tichelaar, E. Aret, and P. R. Hageman, J. Appl. Phys. **92**, 3947 (2002).
[11] H. Maiwa and N. Ichinose, Jpn. J. Appl. Phys. **40**, 5507 (2001).
[12] K. Yamakawa, K. W. Gachigi, S. Trolier-McKinstry, and J. P. Dougherty, J. Math. Sci. **32**, 5169 (1997).
[13] I. Kim, S. Bae, K. Kim, H. Kim, J. S. Lee, J. Jeong, and K. Yamakawa, J. Korean Phys. Soc. **33**, 180 (1998).
[14] J. Zhai and H. Chen, Appl. Phys. Lett. **82**, 2673 (2003).
[15] K. Boldyreva, D. Bao, G. L. Rhun, L. Pintilie, M. Alexe, and D. Hesse, J. Appl. Phys. **102**, 044111 (2007).
[16] R. W. Whatmore and A. M. Glazer, J. Phys C **12**, 1505 (1979).
[17] U. V. Waghmare and K. M. Rabe, Ferroelectrics **194**, 135 (1997).
[18] K. Leung, E. Cockayne, and A. F. Wright, Phys. Rev. B **65**, 214111 (2002).
[19] D. J. Singh, Phys. Rev. B **52**, 12559 (1995).
[20] H. Fujishita and S. Katano, J. Phys. Soc. Jpn. **66**, 3484 (1997).
[21] M. D. Johannes and D. J. Singh, Phys. Rev. B **71**, 212101 (2005), and references therein.
[22] D. L. Corker, A. M. Glazer, R. W. Whatmore, A. Stallard, and F. Fauth, J. Phys.: Condens. Matter **10**, 6251 (1998).
[23] K. Boldyreva, L. Pintilie, A. Lotnyk, I. B. Misirlioglu, M. Alexe, and D. Hesse, Appl. Phys. Lett. **91**, 122915 (2007).
[24] A. Y. Liu and D. J. Singh, Phys. Rev. B **47**, 8515 (1993).
[25] Z. Wu and R. E. Cohen, Phys. Rev. Lett. **95**, 037601 (2005).
[26] S. Ikegami, I. Ueda, and T. Nagata, J. Acoust. Soc. Am. **50**, 1060 (1971).
[27] F. Jona, G. Shirane, and R. Pepinsky, Phys. Rev. **97**, 1584 (1955).
[28] G. R. Bai, H. L. M. Chang, D. J. Lam, and Y. Gao, Appl. Phys. Lett. **62**, 1754 (1993).
[29] W. Kohn and L. J. Sham, Phys. Rev. **140**, A1133 (1965).
[30] L. Hedin and B. I. Lundqvist, J. Phys. C **4**, 2064 (1971); D. M. Ceperley and B. J. Alder, Phys. Rev. Lett. **45**, 566 (1980); J. P. Perdew and A. Zunger, Phys. Rev. B **23**, 5048 (1981); We have used the Hedin-Lundqvist and the Ceperley-Alder (as parametrized by Perdew and Zunger) exchange-correlation functionals for our in-house (LAPW method) and SIESTA codes, respectively.
[31] D. J. Singh and L. Nordstrom, *Planewaves, Pseudopotentials, and the LAPW Method*, 2nd ed. (Springer, New York, 2006).
[32] D. J. Singh, Phys. Rev. B **43**, 6388 (1991).
[33] R. D. King-Smith and D. Vanderbilt, Phys. Rev. B **47**, 1651 (1993).
[34] J. M. Soler *et al.*, J. Phys.: Condens. Matter **14**, 2745 (2002); P. Ordejón, E. Artacho, and J. M. Soler, Phys. Rev. B **53**, R10441 (1996); D. Sánchez-Portal *et al.*, Int. J. Quantum Chem. **65**, 453 (1997).
[35] N. Troullier and J. L. Martins, Phys. Rev. B **43**, 1993 (1991); L. Kleinman and D. M. Bylander, Phys. Rev. Lett. **48**, 1425 (1982); X. Gonze, R. Stumpf, and M. Scheffler, Phys. Rev. B **44**, 8503 (1991).
[36] H. J. Monkhorst and J. D. Pack, Phys. Rev. B **13**, 5188 (1976).
[37] L. Fast, J. M. Wills, B. Johansson, and O. Eriksson, Phys. Rev. B **51**, 17431 (1995); P. Ravindran, L. Fast, P. A. Korzhavyi, B. Johansson, J. Wills, and O. Eriksson, J. Appl. Phys. **84**, 4891 (1998).
[38] H. Fujishita, Y. Ishikawa, S. Tanaka, A. Ogawaguchi, and S. Katano, J. Phys. Soc. Jpn. **72**, 1426 (2003).
[39] J. R. Neighbours and G. E. Schacher, J. Appl. Phys. **38**, 5366 (1967).
[40] J. Chen, L. L. Boyer, H. Krakauer, and M. J. Mehl, Phys. Rev. B **37**, 3295 (1988); M. J. Mehl, *ibid.* **47**, 2493 (1993); J. E. Osburn, M. J. Mehl, and B. M. Klein, *ibid.* **43**, 1805 (1991); Y. Le Page and P. Saxe, *ibid.* **63**, 174103 (2001).
[41] J. F. Nye, *Physical Properties of Crystals* (Oxford University Press, New York, 1985).
[42] G. A. Saunders, Y. K. Yogurtcu, J. E. Macdonald, and G. S. Pawley, Proc. R. Soc. London, Ser. A **407**, 325 (1986).
[43] O. L. Anderson, J. Phys. Chem. Solids **27**, 547 (1966).
[44] A. Y. Wu and R. J. Sladek, Phys. Rev. B **27**, 2089 (1983).
[45] H. M. Ledbetter and D. T. Read, J. Appl. Phys. **48**, 1874 (1977).
[46] M. J. P. Musgrave, *Crystal Acoustics* (Holden-Day, San Francisco, 2003).